CRACKING AND LOCAL MELTING IN Mg-ALLOY AND Al-ALLOY DURING FRICTION STIR SPOT WELDING




M. Yamamoto [a1] A. Gerlich [b2] T.H. North [b3] K. Shinozaki [a4]

[a] Graduate School of Engineering, Hiroshima University (Japan)
[b] University of Toronto, Dept. of Materials Science and Engineering (Canada)
E-mail: [1] motoyama@hiroshima-u.ac.jp, [2] gerlich@ecf.utoronto.ca,
[3] north@ecf.utoronto.ca, [4] kshino@hiroshima-u.ac.jp

ABSTRACT

Although it is generally assumed that friction stir seam welds and friction stir spot welds are free of many of the defect formation issues commonly associated with fusion welding, liquid penetration induced (LPI) cracking in the stir zone have been recently found in friction stir spot welds of AZ91. In the present study, cracking during friction stir spot welding of Mg-alloy (AZ91, AM60 and AZ31) sections is examined. Both liquation cracking and liquid penetration induced (LPI) cracking are observed in Mg-alloy friction stir welded joints. Local melting and cracking is also apparent in Al 7075-T6 friction stir spot welds produced with the precise objective of limiting dissolution of melted eutectic films in the high temperature stir zone and when spot welds cool to room temperature. Based on these test results there is no need to assume that the stir zone temperature during friction stir spot welding is less than that required for formation of melted eutectic films or for spontaneous melting of second-phase particles contained in the as-received base material.

IIW-Thesaurus Keywords: *Eutectics; Cracking; Defects; Friction stir welding; Friction welding; Melting; Reference lists.*

1 INTRODUCTION

There is much interest in the application of Mg-alloy and Al-alloy components during automotive manufacture since lighter base materials provide significant reductions in weight. However, fusion welding of Mg-alloys and Al-alloy encounters the following problems, e.g. hydrogen porosity and increased distortion, solidification cracking and liquation cracking [1-4].

Friction stir spot welding attracts a lot of attention in the fabrication of Mg-alloy and Al-alloy components since it is generally assumed that friction stir seam welding and friction stir spot welding are the perfect solid-state welding processes. Therefore, it is also assumed that the highest temperatures produced within the stir zone during friction stir seam welding and friction stir spot welding are much less than those required for melting. However, North and Gerlich *et al*. [5-15] have already proposed and confirmed that the highest temperature attained in the stir zones of Al-alloy and Mg-alloy friction stir spot welds is ultimately limited by either the solidus temperature of the alloy in question or the spontaneous melting temperatures of second-phase particles, which are contained in the as received base material. For example, the highest temperatures found in the stir zones of Al 7075, Al 2024, Al 6111, Al 6061, Al 5754, AZ31, AZ91 and AM50 friction stir spot welds correspond with their solidus temperature (Ts in Kelvin) ranging from 0.94 Ts to 0.99 Ts [5-15]. When AZ91

Doc. IIW-1867-07 (ex-doc. III-1429r1-07) recommended for publication by Commission III “Resistance welding, solid state welding and allied joining processes”.

base material is spot welded, the temperature in the stir zone at the end of the 4 second long dwell period (438 °C) is remarkably close to the (α-Mg + $Mg_{17}Al_{12}$) eutectic temperature in the Al-Mg binary equilibrium diagram (437 °C) [16]. On the other hand, much higher temperatures (525 °C and 550 °C) are found in AM60 and AZ31 friction stir spot welds [8].

In addition, although it is generally assumed that friction stir seam welds and friction stir spot welds are free of many of the defect formation issues commonly associated with fusion welding, liquid penetration induced (LPI) cracking has been recently found in the stir zones of AZ91 friction stir spot welds [16-18]. Yamamoto [8] proposed that LPI cracking in AZ91 friction stir spot welds is determined by the following factors:

i) Stir zone and TMAZ temperatures ≥ 437 °C during the dwell period in spot welding [this is the (α-Mg + Mg17Al12) eutectic temperature in the Al-Mg binary equilibrium phase diagram].

ii) The formation of melted eutectic films in the TMAZ region early in the dwell period during spot welding in the location immediately adjacent to the stir zone extremity.

iii) The engulfment of melted eutectic films as the stir zone grows in width during the dwell period. Although subsequent dissolution of melted eutectic film occurs, this facilitates penetration of equiaxed α-Mg grain boundaries within the stir zone close to its extremity.

iv) Crack propagation when torque is applied by the tool as it rotates during the dwell period in spot welding.

The present paper examines the cracking mechanism during friction stir spot welding of Mg-alloys (AZ91, AM60 and AZ31) and an Al-alloy (Al 7075) in detail. The cracking tendency has been defined as the amount of stir zone material created during the spot welding operation that is removed when the rotating tool is retracted at any dwell time setting [8, 16]. The crakking tendency is readily determined by measuring the change in mass of AZ91 test specimens before and following tool withdrawal. This measurement technique is employed in the present study to investigate the failure propensities at the locations close to the pin periphery and close to the stir zone extremity in AZ91 spot welds. The microstructures and failure propagation through the stir zone are examined in welds made using different dwell time settings.

2 EXPERIMENTAL PROCEDURE

Friction stir spot welding of Mg-alloy sections was carried out using 3 mm to 8 mm thick x 25 mm diameter sections of a thixomolded AZ91 (Mg 9wt %Al 0.7wt %Zn) extrusion, 2.6 mm thick sections of thixomolded AM60 (Mg 6wt %Al 0.4wt %Mn) sheets and 2.6 mm thick sections of a wrought AZ31 (Mg 3wt %Al 1wt %Zn) sheet. Friction stir spot welding of Al-alloy sections was carried out using 1.5 mm and 5 mm thick sections of Al 7075-T6 (Al 0.2wt %Cr 1.3wt %Cu 2.3wt %Mg 5.4wt %Zn) sheets.

The spot welding equipment employed in the present investigation had a rotational speed capability up to 3 000 rpm while a servomotor provides axial loads up to 12 kN. The amount of tool penetration (displacement) during spot welding was measured using a linear transducer with an accuracy of ± 0.01 mm. The axial load and torque were measured using a JR3 six-axis load cell, which is coupled to a data acquisition system.

Spot welding was carried out using a H13 tool steel having a hardness of 46-48 HRC. The shoulder diameter was 10 mm, the pin diameter was 4 mm and the pin length was 2.2 mm. The pin had a threaded geometry corresponding with an M4 metric screw profile and during the spot welding operation the tool rotated in a counterclockwise direction. Plunge rates as high as 25 mm/s were selectable during friction stir spot welding, with the penetration depth being attained with an accuracy of ± 0.1 mm.

The thermal cycle in the stir zone during friction stir spot welding was measured by embedding 0.25 mm diameter K-type thermocouples at the location 0.20 mm from the tip of the rotating pin and 1.3 mm from the outer periphery of the tool shoulder, see Figure 1. During all temperature measurements the thermocouple junction was always in direct contact with dynamically recrystallized material formed during the spot welding operation. A detailed description of the temperature measurement set-up was provided elsewhere [5]. The variation in temperature during the 4 second dwell period was < 7.4 °C during repeat testing.

The thermal cycles in TMAZ and HAZ regions during spot welding were measured by locating thermocouples of 0.25 mm diameter at a distance of 2 to 4 mm from the pin periphery before spot welding, as shown in Figure 2. In all cases the tips of the drilled holes were set level with the bottom of keyhole while the exact locations of the thermocouples relative to the bottom of the shoulder and to the periphery of the rotating pin were determined by sectioning and metallographic examination.

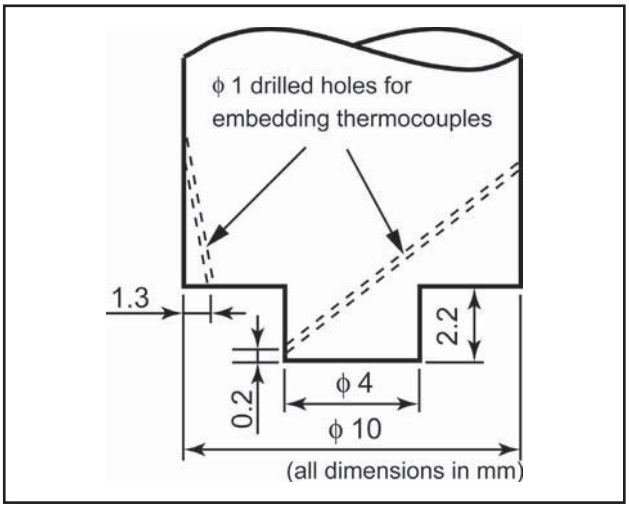

Figure 1 – Thermocouple locations within the tool itself

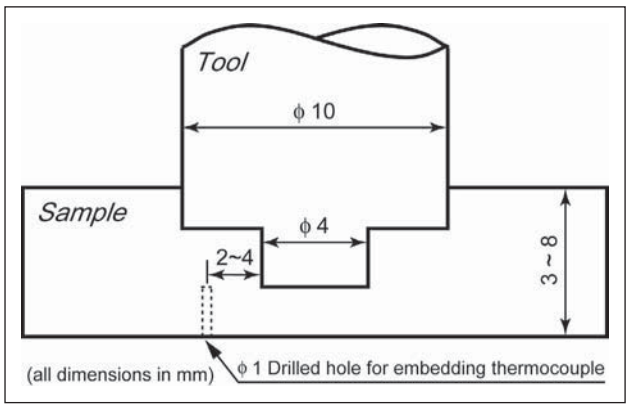

Figure 2 – Thermocouple locations within the sample

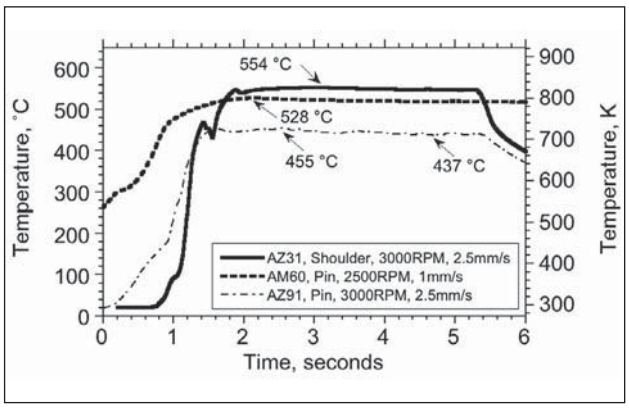

Figure 3 – Temperature outputs during spot welding of AZ91, AM60 and AZ31

Spot welding of room temperature and rapidly-quenched test sections was investigated. Rapid cooling of AZ91 test specimens was facilitated by immersing them in a mixture of methanol and liquid nitrogen at a temperature of -80 °C and spot welding using a rapid plunge rate of 25 mm/s. Tool rotation was terminated at selected dwell time settings during spot welding and both the steel tool and the adjacent stir zone material were sectioned prior to metallographic examination. Local melting and cracking during Al 7075-T6 spot welding was investigated in joints made using a plunge rate of 10 mm/s, an extremely short dwell time (0.25 s) followed by rapid quenching of spot welded samples.

The microstructural changes during the tool penetration stage and the subsequent dwell period in spot welding were examined. The metallographic features of Mg-alloys were investigated following etching in either 5 vol. % nital solution and/or acetic-picral solution comprising 10 ml acetic acid, 4.2 g picric acid, 10 ml H_2O and 70 ml of 95 vol. % ethanol. Al 7075-T6 spot welds were examined using Keller's reagent.

The cracking tendency during LPI cracking has been defined as the amount of the stir zone material created during spot welding, which is removed when the rotating tool is withdrawn at any dwell time setting and could be readily evaluated by measuring the mass of the AZ91 test samples prior to and following friction stir spot welding [8, 16]. The amount of material removed by the rotating tool when it is retracted at different dwell time settings was determined by weighing the AZ91 sections before and after spot welding using a Mittler Toledo International Inc. AE160 weighing machine having an accuracy of ±0.01 mg.

3 RESULTS AND DISCUSSION

3.1 Stir zone temperature

The stir zone temperature approaches the solidus temperature in the stir zone of AZ91, AZ31 and AM60 friction stir spot welds, see Figure 3. In AZ91 spot welds, for example, the measured stir zone temperature early in the dwell period (455 °C) is close to the solidus temperature of AZ91 (470 °C). At the end of the dwell period in AZ91 spot welding the temperature decreases to 437 °C, corresponding with the α-Mg + (α-Mg + $Mg_{17}Al_{12}$) eutectic temperature in the binary Al-Mg equilibrium phase diagram. The highest stir zone temperatures during AZ91, AM60 and AZ31 spot welding correspond with homologous temperatures of 0.98, 0.99 and 0.94, see Figure 3.

It has been confirmed recently that the temperature within the stir zone cannot be determined by embedding thermocouples in drilled holes within 0.5 mm from the periphery of the rotating pin prior to spot welding since the helical vertical rotational flow set-up within the stir zone formed adjacent to the periphery of the rotating pin displaces the thermocouples from their original locations [18, 19]. The most effective means of measuring the temperature during friction stir spot welding involves locating the thermocouples within the tool itself. However, even when this methodology is employed, the measured temperature values are likely less than the actual values at the contact interface [15].

3.2 LPI cracking mechanism

Figure 4 shows the temperature cycles measured in the TMAZ region close to the extremity of the stir zone during AZ91, AM60 and AZ31 spot welding. It is worth noting here that although the temperature in the TMAZ region can be measured by embedding thermocouples into the test samples prior to spot welding it is difficult if not impossible to obtain consistent temperature out-

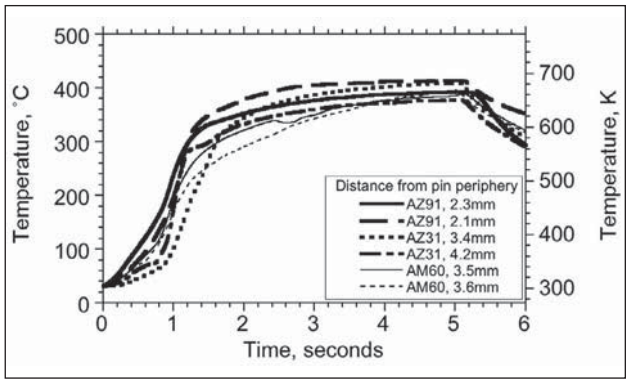

Figure 4 – Temperature outputs in the TMAZ region during spot welding of AZ91, AM60 and AZ31

put at a pre-selected location relative to the stir zone extremity [18].

Figure 5 shows metallographic evidence confirming melted eutectic formation and cracking in the TMAZ regions of AZ91, AM60 and AZ31 spot welds made using very short dwell time settings. In AZ91 friction stir spot welds the melted eutectic films are engulfed when the stir zone grows in size during the dwell period and this facilitates penetration of α-Mg grain boundaries within the stir zone close to its extremity, see Figure 6. It can be assumed that crack propagation occurs when torque is applied as the tool rotates during the spot welding dwell period [8, 16, 20, 21]. Melted eutectic films are rapidly heated to the stir zone temperature when they are engulfed by the growing stir zone.

During AM60 and AZ31 friction stir spot welding the stir zone temperatures (525 °C and 550 °C) are much higher than the eutectic temperature (437 °C) and as a result, there is a strong tendency for melted eutectic films to dissolve rapidly immediately following their engulfment by the expanding stir zone. The rapid dissolution of melted eutectic films formed in the TMAZ region during AM60 and AZ31 spot welding explains why crack-free spot welds are produced using a dwell time of 4 seconds, see Figure 7 a). In contrast, the stir zone temperature is close to 437 °C at the end of the dwell period in AZ91 spot welding and, although some dissolution of melted eutectic films occurs, LPI cracking is still observed in spot welds produced using a dwell time of 4 seconds, see Figure 7 b). Since the dissolution kinetics of melted eutectic films and melted droplets is extremely important during friction stir spot welding, this particular aspect will be discussed in detail.

The dissolution kinetics of melted eutectic films have been evaluated by Reiso *et al*. [22] during upquenching of Al-alloy sections and by Gerlich *et al*. [5, 6] and Yamamoto *et al*. [8, 16] during friction stir spot welding of Al 7075, Al 2024, AZ91, AM60 and AZ31. The dissolution of plate-shaped liquid films is determined by the relation:

$$B = B_0 - \frac{k}{\sqrt{\pi}}\sqrt{Dt} \quad (1)$$

$$t = \frac{\pi B_0^2}{Dk^2} \quad (2)$$

where

B is half the thickness of the liquid film, and

B_0 is half the initial film thickness.

The dissolution kinetics of liquid droplets during spot welding are determined by a range of factors:

a) The spontaneous melting temperature. This is 437 °C (710 K) during AZ91 friction stir spot welding.

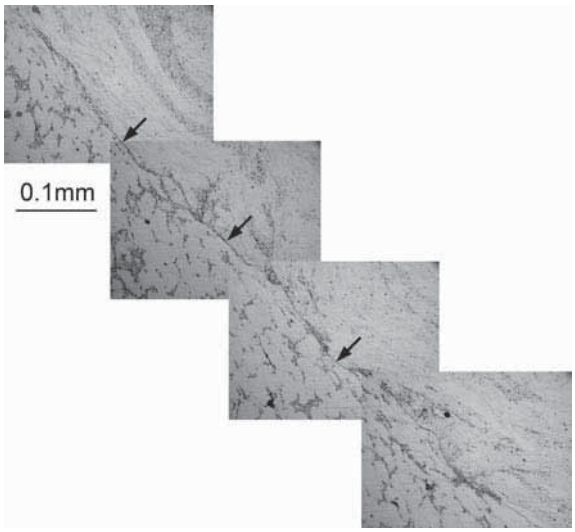

a) AZ91, at the location immediately adjacent to the stir zone, Dwell time: 0.1 s

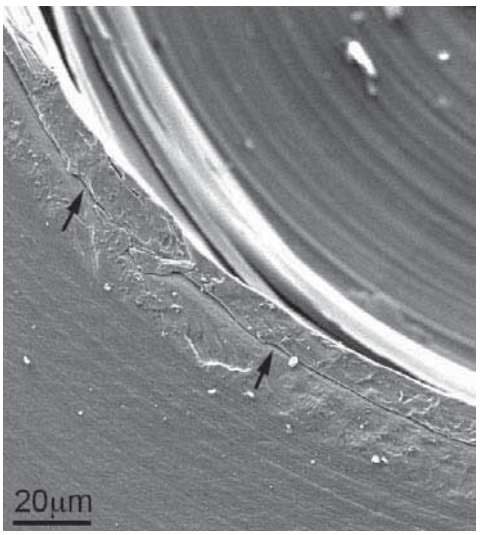

c) AZ31, at the edge of the keyhole, Dwell time: 0.05 s

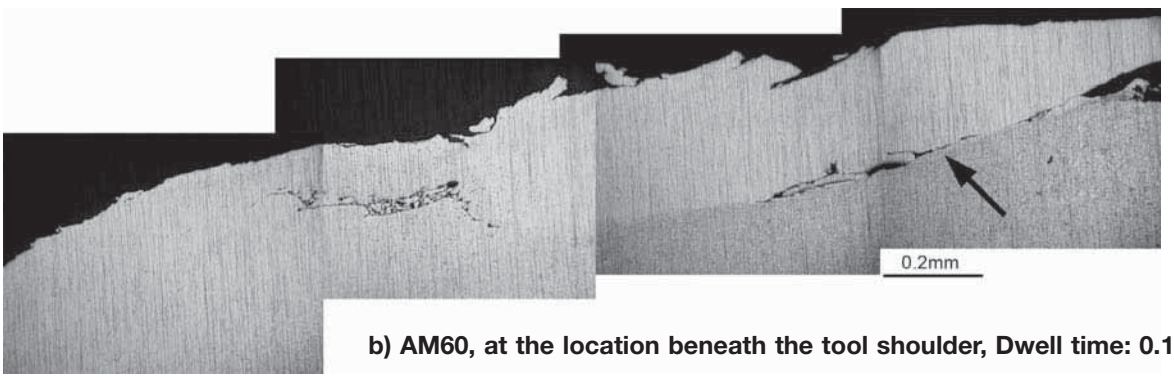

b) AM60, at the location beneath the tool shoulder, Dwell time: 0.1 s

Figure 5 – Cracking in the TMAZ region during spot welding of AZ91, AM60 and AZ31 using a tool rotational speed of 3 000 rpm and a plunging rate of 25 mm/s

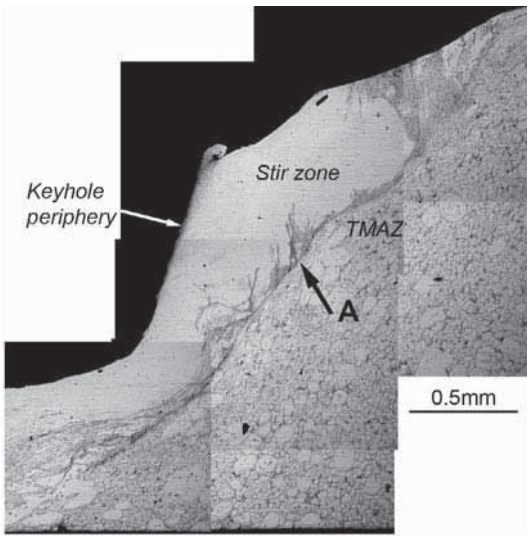

a) Penetration and cracking at grain boundary regions in the stir zone at the location close to its extremity in AZ91 spot welds made using a tool rotational speed of 3 000 pm, plunge rate of 25 mm/s and a dwell time of 0.25 seconds

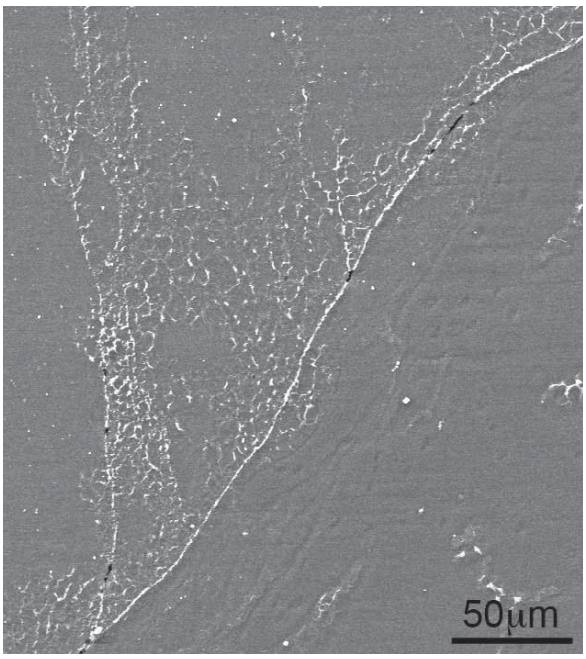

b) SEM observation at the location A in a)

Figure 6

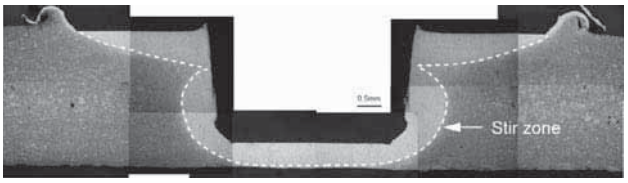

a) AM60

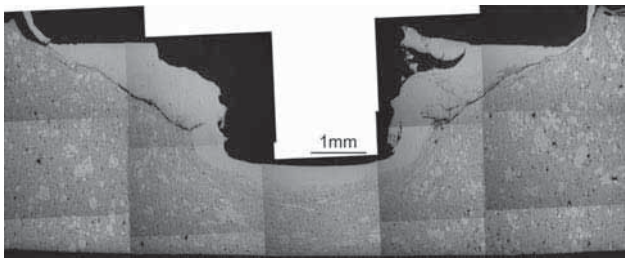

b) AZ91

Figure 7 – The spot weld profiles produced using a tool rotational speed of 3 000 rpm, plunge rate of 25 mm/s and a dwell time of 4 seconds

b) The diffusion coefficient of solute atoms at the stir zone temperature.

c) The thermodynamic driving force for diffusion and dissolution.

d) The shape and dimensions of the liquid droplets, which is determined by the dimensions and particle size distribution of second-phase particles in the as-received material and by thermo-mechanical deformation during the tool penetration stage in spot welding.

e) The time available for dissolution during the dwell period in spot welding and when the spot weld cools to room temperature.

The above dissolution calculations assume that the melted droplets are suspended in a quiescent matrix. No account is taken of the fact that

i) α-Mg grains are elongated and $Mg_{17}Al_{12}$ particles are aligned in the TMAZ region due to the thermo-mechanical deformation applied during tool penetration, and

ii) stir zone material is being constantly sheared and strained as the tool rotates during the dwell period in spot welding [6, 8, 16].

Figure 8 shows the dissolution kinetics of melted droplets formed in the stir zones during AZ91, AM60 and AZ31 friction stir spot welding. The dissolution rate is much slower during the dwell period in AZ91 spot welding. For example, when the temperature of 437 °C is assumed, a 90 nm thick film of melted eutectic will dissolve in about 4 seconds. Since 0.5 μm to 1.5 μm thick $Mg_{17}Al_{12}$ films are observed at α-Mg grain boundary regions in the stir zone close to its extremity, it would

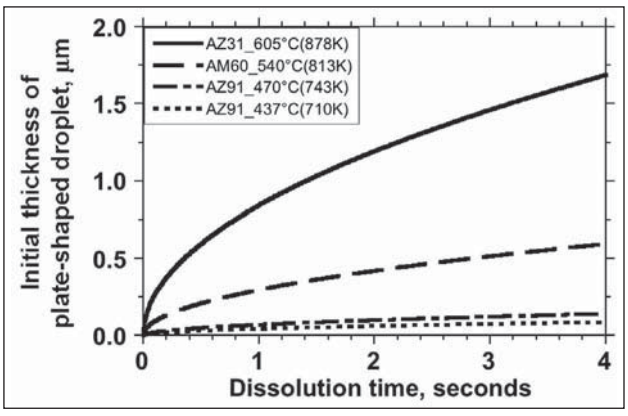

Figure 8 – Relation between the width of a plate-shaped film of melted eutectic and the dissolution time when solidus and eutectic temperatures of 437 °C and 470 °C (AZ91), 540 °C (AM60) and 605 °C (AZ31) are assumed

be expected that AZ91 friction stir spot welds made using a dwell time of 4 seconds would exhibit LPI cracking. However, the dissolution rate of eutectic films is much more rapid during AM60 and AZ31 spot welding since much higher stir zone temperatures are produced. Following their engulfment by the growing stir zone melted eutectic films are rapidly dissolved and although TMAZ cracking is apparent early in the dwell period (in spot welds made using dwell times of 0.05 and 0.1 seconds) crack-free spot welds are produced when a dwell time of 4 seconds is applied [8].

3.3 Cracking tendency during AZ91 spot welding

Yamamoto [8, 16] used a mass removal technique to monitor the LPI cracking tendency in AZ91 spot welds. The cracking tendency is defined as the mass of the stir zone created during the spot welding operation, which is removed by the rotating tool when it was withdrawn. Figure 9 shows the relation between the mass of material removed when the rotating tool is withdrawn and the dwell time during AZ91 spot welding. Although there is scatter in the test output at all dwell period, it can be seen from Figure 9 that the mass of stir zone material removed by the rotating tool is highest when the dwell time increases to around 2 seconds and then the weight loss of some specimens decreases. It can also be seen from Figure 9 that there is the most considerable scatter in testing output when a dwell time of 4 seconds is applied. Increased scatter results when the mode of failure during tool withdrawal switches from failure in the location close to the stir zone extremity to failure in the location close to the periphery of the rotating pin, see Figures 10 a) and 10 b). It is readily apparent from Figure 10 a) that almost the entire stir zone is removed by the rotating tool when preferential failure occurs close to the extremity of the stir zone during AZ91 spot welding. When preferential failure occurs coincident with the keyhole periphery much less stir zone material is removed, see Figures 9 and 10 b). The change from preferential

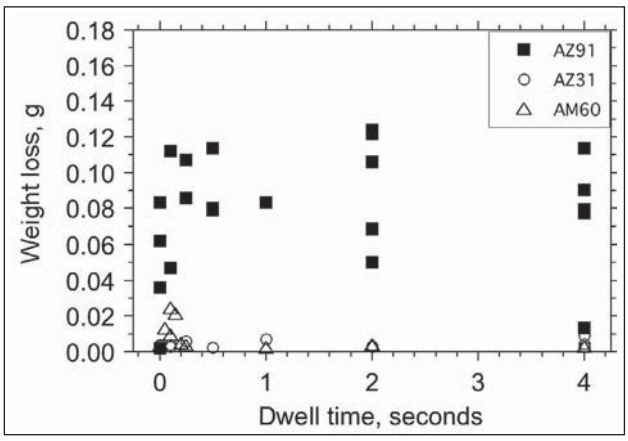

The plunge rate was 25 mm/s and the tool rotational speed was 3 000 rpm.

Figure 9 – Amount of stir zone material removed when the rotating tool is withdrawn for different dwell times during AZ91, AZ31 and AM60 spot welding

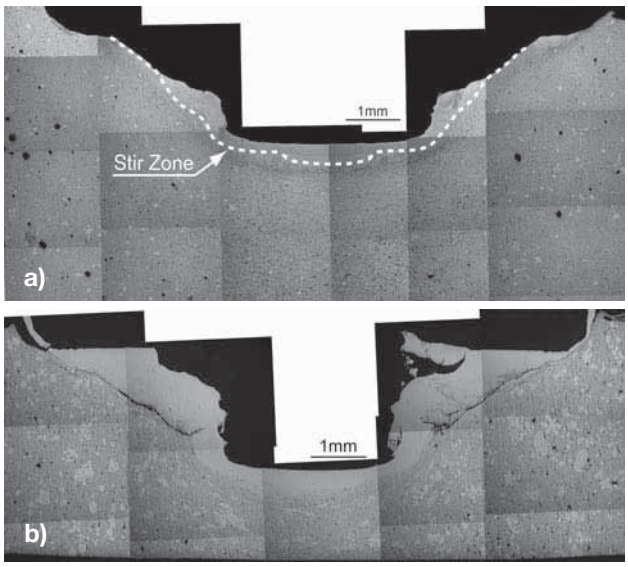

Figure 10 – Failure profiles produced during AZ91 spot welding using a dwell time of 4 seconds, a rotational speed of 3 000 rpm and a plunging rate of 25 mm/s

failure close to the stir zone extremity to preferential failure coincident with almost the entire length of the rotating pin is promoted by the formation of melted eutectic material at the root of the pin thread, see Figure 11.

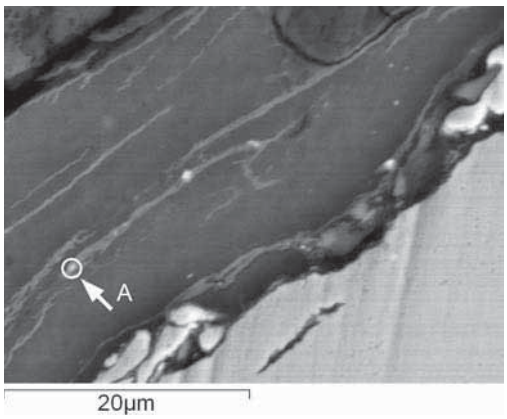

a) Spot weld made using dwell time of 0.75 seconds

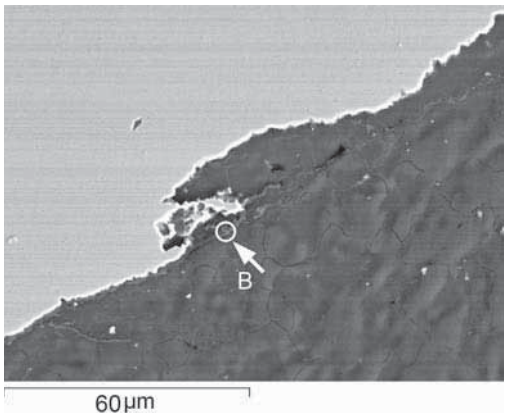

b) Spot weld made using dwell time of 2.9 seconds

The chemical composition at locations A in a) and B in b) are 71.1 wt %Mg, 21.6 wt %Al and 72.8 wt %Mg, 22.3 wt %Al respectively. The plunge rate was 25 mm/s and the tool rotational speed was 3 000 rpm, and the tool rotation was suddenly terminated during spot welding.

Figure 11 – Eutectic formation at the root of the pin thread in AZ91 spot welds

Figure 12 shows the cracking under the shoulder when rapidly-quenched AZ91 spot welds made using dwell times of 0.25 s, 0.75 s, 1.25 s and 2.9 s are examined. In each case the AZ91 test sections were held at -80 °C prior to spot welding and tool rotation was suddenly terminated during spot welding operations as explained in the experimental procedure section.

Figure 12 a) shows extensive cracking in the location beneath the tool shoulder in an AZ91 spot weld made using a dwell time of 0.25 s. A highly-deformed α-Mg microstructure containing thin veins of melted eutectic material is formed in the location beneath the tool shoulder, see Region A in Figure 12 a). For example, location B in Figure 12 b) has a chemical composition closely corresponding with the (α-Mg + $Mg_{17}Al_{12}$) eutectic composition in the binary Al-Mg equilibrium phase diagram. It has already been confirmed that the temperature exceeds the (α-Mg + $Mg_{17}Al_{12}$) eutectic temperature (437 °C) very early in AZ91 spot welding when a plunge rate of 25 mm/s and a tool rotational speed of 3 000 rpm are employed [5]. Region A in Figure 12 a) is heated during the pin penetration process, when material from beneath the tip of the rotating pin is displaced upwards during pin penetration and when material is trapped between the base of the rotating tool shoulder and the upper surface of the AZ91 section [16]. It is therefore suggested that a funnel-shaped region comprising high-deformed material rich in eutectic forms

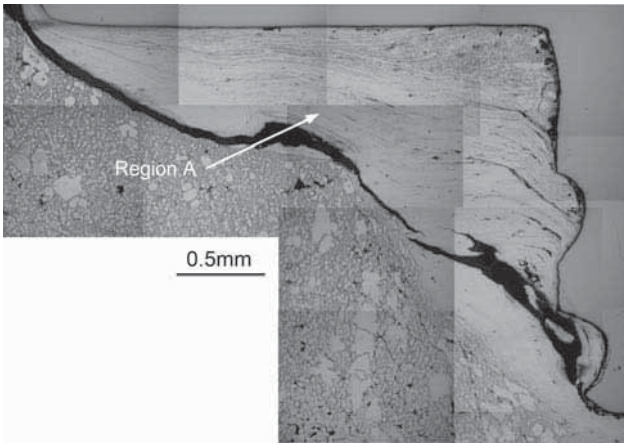

a) Spot weld made using dwell time of 0.25 seconds

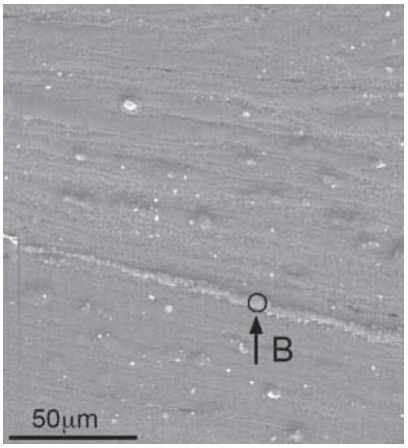

b) Spot weld made using dwell time of 0.25 seconds

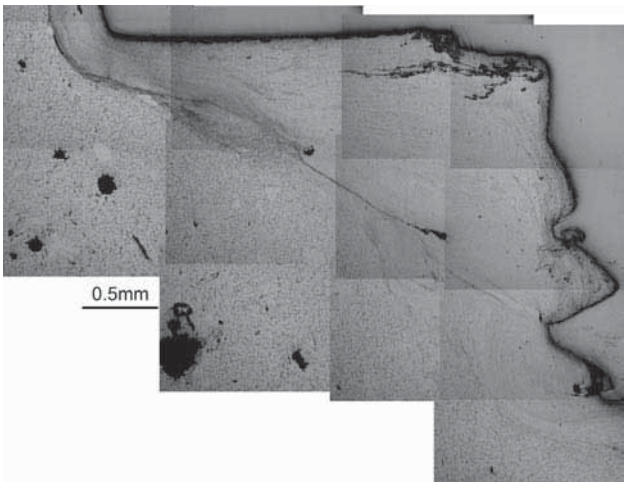

c) Spot weld made using dwell time of 0.75 seconds

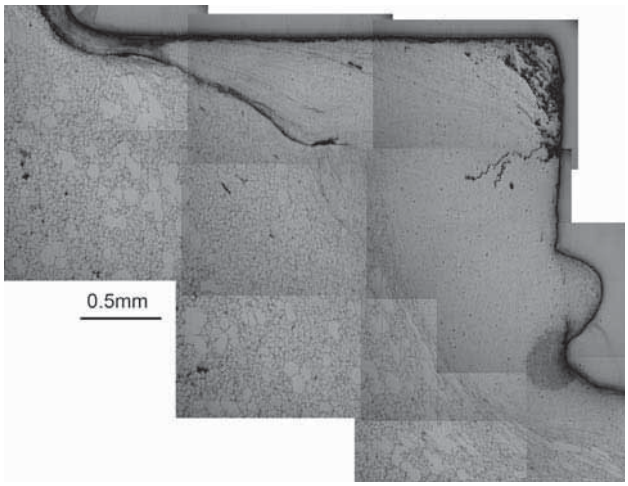

d) Spot weld made using dwell time of 1.25 seconds

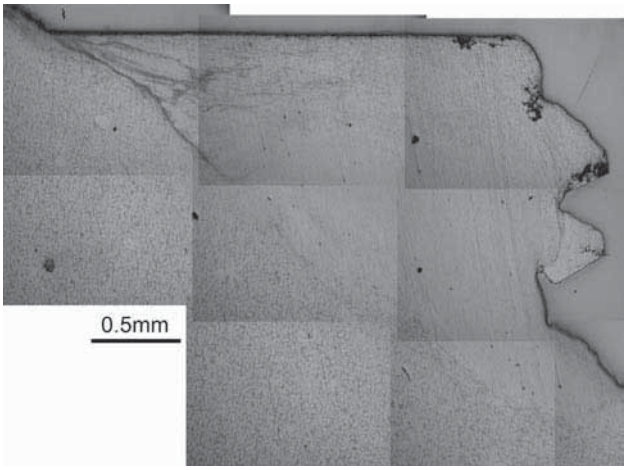

e) Spot weld made using dwell time of 2.9 seconds

Figure b) shows an SEM image of location A in Figure a). The chemical composition at location B in Figure b) is 70.8 wt.% Mg, 29.2 wt.% Al in spot welds made using a plunge rate of 25 mm/s and a tool rotational speed of 3 000 rpm. The test samples were at -80 °C prior to spot welding and tool rotation was suddenly terminated.

Figure 12 – Cracking in the location beneath the tool shoulder in AZ91 spot welds

beneath the tool shoulder very early in the AZ91 spot welding operation. The cracking shown in Figure 12 a) therefore represents the boundary between material rich in melted eutectic that is rotating with the tool and material, which is not rotating.

The size of the funnel-shaped region containing eutectic material decreases when the dwell time is extended, see Figures 12 a) to 12 e) since melted eutectic material, which promotes crack formation, dissolves. The length of the crack formed in the location beneath the tool shoulder is consequently decreased when the dwell time increases from 0.25 s to 2.9 s. In this connection, Yamamoto [8, 16] examined the circumferential displacement of material expelled from the periphery of the tool shoulder during the dwell period in AZ91 spot welding. Circumferential displacement of expelled material from the periphery of the tool shoulder occurred early in the dwell period and then ceased when the dwell time increased beyond around 2 seconds. With this in mind, the results shown in Figures 12 a) to 12 e) are consistent with the proposal that Yamamoto's high-speed imaging output resulted from cracking in the location beneath the tool shoulder.

The mass removal technique developed by Yamamoto [8, 16] provides a straightforward, inexpensive and permits rapid means of determining the likelihood of encountering cracking problems during friction stir spot welding when dwell times less than about 2 seconds. However, when the dwell time exceeds about 2 seconds the mode of failure during tool retraction can change so that much less stir zone material than expected is removed.

3.4 Eutectic melting and cracking in Al 7075-T6 spot welds

Figure 13 shows the location immediately beneath the tool shoulder in a rapidly quenched Al 7075 spot weld made using a tool rotational speed of 3 000 rpm, a plunge rate of 10 mm/s and an extremely short dwell time (0.05 seconds). The local melted eutectic films in Figure 13 b) are etched preferentially by Keller's reagent and are rich in Zn and Cu. It is worth noting that the formation of Cu and Mg-rich films at grain boundary regions has already been associated with local melting in the stir zones of Al 7010 and Al 2024/SiC friction stir seam welds.

It must be emphasized the melted films shown in Figure 13 are retained in Al 7075 spot welds precisely because measures are taken to prevent dissolution of melted eutectic material during the friction stir spot welding operation. Figure 14 compares the dissolution kinetics of plate-shaped melted droplets in the stir zones produced during Al 7075 and AZ91 spot welding. Spontaneous melting occurs when the welding parameter settings produce stir zone temperatures ≥ 475 °C during Al 7075-T6 spot welding [5]. Since as-received Al 7075-T6 sheet contains 60 nm thick x 120 nm long second-phase particles (η, S and T phase) it is readily apparent that there will be a considerable tendency for 100 nm thick plate-shaped melted droplets to dissolve during the dwell period in spot welding, see Figure 14. Particle

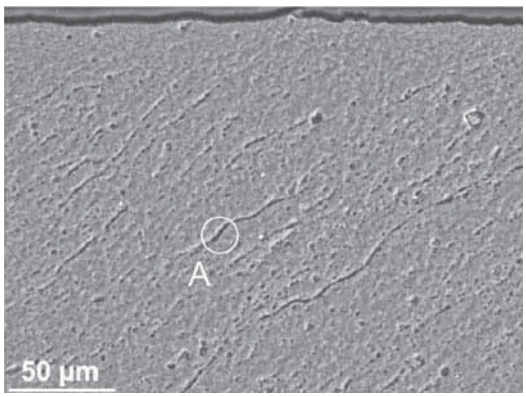

a) SEM micrograph showing the melted eutectic films

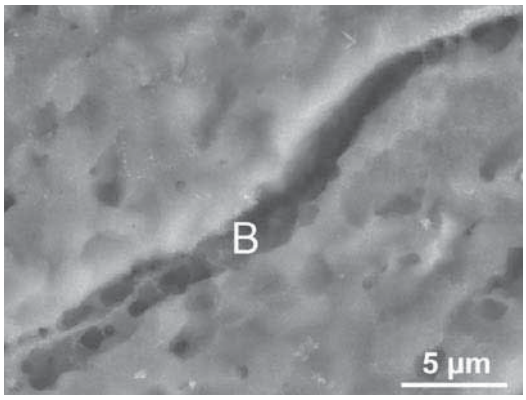

The chemical composition at location A is 83.4 wt %Al, 10.0 wt %Zn, 4.7 wt %Cu, 2.0 wt % Mg.

b) Detail showing the melted film at the location A in a) and EDX chemical analysis at location B

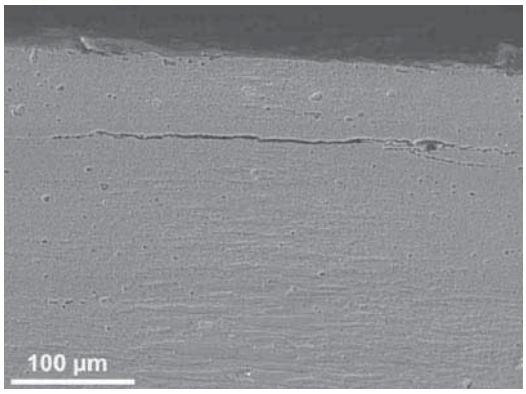

c) Cracking in the location close to the tip of the rotating pin

Figure 13 – Melted films observed in an Al 7075 friction stir spot weld made using a plunge rate of 10 mm/s, a dwell time of 0.05 s and a tool rotation speed of 3 000 rpm

dissolution will also continue when Al 7075 friction stir spot welds cool to room temperature. With this in mind, metallographic evidence confirming melted film formation during Al 7075-T6 spot welding will only be found when steps are taken to limit the dissolution process.

An extremely short dwell time (0.05 seconds) and a high plunge rate are used in addition to rapid quenching immediately when the spot welding operation is terminated. Unless steps of this nature are taken dissolution during the dwell period and as Al 7075-T6 spot weld cool to room temperature will remove any evidence of melted film formation. Based on this testing output,

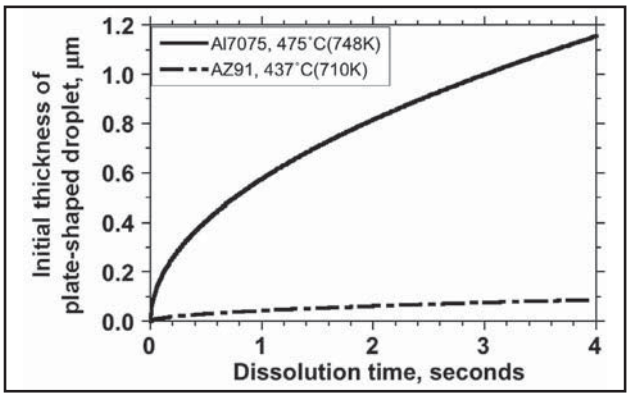

Figure 14 – The dissolution kinetics of plate-shaped liquid droplets formed in the stir zones of Al 7075-T6 and AZ91 spot welds

Al 7075-T6 friction stir spot welds do exhibit local melting and cracking very early in the dwell period in spot welding and all evidence of their occurrence is removed when the dwell period continues and completed spot welds cool to room temperature. It follows that there is no need to assume that the temperature attained in the stir zone during friction stir spot welding is less than that required for formation of melted eutectic films or for spontaneous melting of second-phase particles contained in the as-received base material. Dissolution of melted films in the high temperature stir zone and as completed welds cool to room temperature can readily account for the production of crack-free spot welds.

4 CONCLUSIONS

Melted eutectic film formation and cracking in Mg-alloy friction stir spot welds have been examined. Both liquation cracking and liquid penetration induced (LPI) cracking are observed in friction stir welded joints.

Evidence of local melting and cracking is also apparent in Al 7075-T6 friction stir spot welds produced with the precise objective of limiting dissolution if melted eutectic films in the high temperature stir zone and as completed spot welds cool to room temperature. There is no need to assume that the temperature attained in the stir zone during friction stir spot welding is lower than that required for formation of melted eutectic films or for spontaneous melting of second-phase particles contained in the as received base material.

REFERENCES

[1] ASM Specialty Handbook, Magnesium and Magnesium Alloys, ASM International, 1999, pp. 106-118.

[2] Lathabai S., Barton K.J., Harris D., Lloyd P.G., Viano D.M., McLean A.: Welding and weldability of AZ31B by gas tungsten arc and laser beam welding processes, Magnesium Technology 2003, TMS, 2003, pp. 157-162.

[3] Stern A., Munitz A., Kohn G.: Application of welding technologies for joining of Mg alloys: Microstructure and mechanical properties, Magnesium Technology 2003, TMS, 2003, pp. 163-167.

[4] Tanaka M.: Report of study group for high efficiency welding processes of thin sheet plate, J. Japan Welding Soc., 2004, 74-5, 358.

[5] Gerlich A., Avramovic-Cingara G., North T.H.: Stir zone microstructure and strain rate during Al 7075-T6 Friction Stir Spot Welding, Met. Trans. A., 2006, Vol. 37A, pp. 2773-2786.

[6] Gerlich A., Su P., Yamamoto M., North T.H.: Effect of welding parameters on the strain rate and microstructure of friction stir spot welded 2024 aluminum alloy, J. Mat. Sci., 2007, on-line.

[7] Gerlich A., Su P., North T.H.: Friction stir spot welding of Mg-alloys for automotive applications, in “Magnesium Technology 2005”, 2005, eds. N. R. Neelameggham, H. I. Kaplan and B. R. Powell, TMS, pp. 383-388.

[8] Yamamoto M., Gerlich A., North T.H., Shinozaki K.: Cracking in the stir zones of Mg-alloy friction stir spot welds, J. Mat. Sci., 2007, 42, 18, pp. 7657-7666.

[9] Gerlich A., Su P., North T.H.: Peak temperatures and microstructures in aluminium and magnesium alloy friction stir spot welds, Sci. Tech. Weld. Joining, 2005, 10, 6, pp. 647-652.

[10] Gerlich A., Su P., North T.H.: Tool penetration during friction stir spot welding of Al and Mg alloys, J. Mat. Sci., 2005, 40, pp. 6473-6481.

[11] Gerlich A., Su P., North T.H., Bendzsak G.J.: Friction stir spot welding of aluminum and magnesium alloys, Materials Forum, 2005, 29, pp. 290-294.

[12] Su P., Gerlich A., North T.H., Bendzsak G.J.: Energy utilisation and generation during friction stir spot welding, Sci. Tech. Weld. Joining, 2006, 11, 2, pp. 163-169.

[13] Su P., Gerlich A., North T.H., Bendzsak G.J.: Energy generation and stir zone dimensions in friction stir spot welds, SAE Technical Series, 2006-01-0971.

[14] Gerlich A., Yamamoto M., North T.H.: Strain rates and grain growth in 5754 and 6061 friction stir spot welds, Met. Trans. A, 2007, in press.

[15] Gerlich A., Yamamoto M., North T.H.: Local melting and tool slippage during friction stir spot welding of Al-alloys, J. Mat. Sci., Special Edition on Joining Science and Technology, 2007, in press.

[16] Yamamoto M., Gerlich A., North T.H., Shinozaki K.: Mechanism of cracking in AZ91 friction stir spot welds, Sci. Tech. Weld. Joining, 2007,12, 3, pp. 208-216.

[17] Yamamoto M., Su P., Gerlich A., North T.H., Shinozaki K.: Liquid Penetration Induced (LPI) cracking in AZ91 friction stir spot welds, J. Jpn. Welding Soc., 2007, 25, 1, pp. 208-214 (in Japanese).

[18] Yamamoto M., Su P., Gerlich A., North T.H., Shinozaki K.: Eutectic segregation and cracking in AZ91 friction stir spot welds, SAE Technical Series, 2007, 2007-01-1700.

[19] Su P., Gerlich A., North T.H., Bendzsak G.J.: Intermixing in dissimilar friction stir spot welds, Met. Trans. A, 2007, on-line.

[20] Shinozaki K., North T.H., Yamamoto M., Gerlich A., Horie S., Soejima H., Kamiyama H.: Cracking in dissimilar friction stir spot welding of Mg-Alloy AM60/AZ91, Preprints of the National Meeting of Japan Welding Soc., 2007, Vol. 2007f, pp. 75-76 (in Japanese).

[21] Yamamoto M., Gerlich A., North T.H.: Cracking in dissimilar Mg-alloy friction stir spot welds, Science and Technology of Welding and Joining, 2007, To be published.

[22] Reiso O., Øverlie H.-G., Ryum N.: Dissolution and melting of secondary Al_2Cu phase particles in an AlCu Alloy, Met. Trans., 1990, vol. 21A, 1689.